

Injection of oxygenated Persian Gulf Water into the southern Bay of Bengal

Peter M.F. Sheehan¹, Benjamin G.M. Webber^{1,2}, Alejandra Sanchez-Franks³,
Adrian J. Matthews⁴, Karen J. Heywood¹ and P.N. Vinayachandran⁵

¹Centre for Ocean and Atmospheric Sciences, School of Environmental Sciences, University of East Anglia, Norwich, United Kingdom

²Climactic Research Unit, University of East Anglia, Norwich, United Kingdom

³National Oceanography Centre, Southampton, United Kingdom

⁴Centre for Oceanic and Atmospheric Sciences, School of Environmental Sciences & School of Mathematics, University of East Anglia, Norwich, United Kingdom

⁵Centre for Atmospheric and Oceanic Sciences, Indian Institute of Science, Bangalore, India

Key Points:

- Persian Gulf Water injects oxygen into the Bay of Bengal oxygen minimum zone
- Two transport pathways exist: one in the eastern and one in the western Arabian Sea
- The flux of Persian Gulf Water into the Bay of Bengal is enhanced during the south-west monsoon

Corresponding author: Peter Sheehan, p.sheehan@uea.ac.uk

Abstract

Persian Gulf Water (PGW) is an oxygenated, high-salinity water mass that has recently been detected in the Bay of Bengal (BoB). However, little is known about the transport pathways of PGW into the BoB. Ocean glider observations presented here demonstrate the presence of PGW in the southwestern BoB. Output from an ocean re-analysis product shows that this PGW signal is associated with a northward-flowing filament of high-salinity water. Particle tracking experiments reveal two pathways: one in the eastern Arabian Sea that takes a minimum of two years, and another in the western Arabian Sea that takes a minimum of three years. The western pathway connects to the BoB via equatorial currents. The greatest influx of PGW occurs between 82 and 87°E during the southwest monsoon. We propose that injection of PGW to the BoB OMZ contributes to keeping oxygen concentrations in the BoB above the level at which de-nitrification occurs.

Plain-language summary

The Persian Gulf is a hot, shallow sea that acts like a vast salt pan. Consequently, water flowing out of the Gulf has a very high salt concentration; it also has a relatively high dissolved oxygen concentration. This high-salt, high-oxygen signal is distinct to Persian Gulf Water and is largely preserved as Persian Gulf Water spreads in the ocean's interior. In observations collected by an ocean glider, we identify the remnants of this high-salt, high-oxygen signal in the southwestern Bay of Bengal, a region that is notably lacking in dissolved oxygen. Using an ocean model, we identify two pathways taken by Persian Gulf Water between the northern Arabian Sea and the Bay of Bengal: one in the eastern Arabian Sea that takes a minimum of two years; and one in the western Arabian Sea that takes a minimum of three years. Persian Gulf Water arrives in the Bay of Bengal throughout the year, but particularly during the southwest monsoon (June to September). Persian Gulf Water brings oxygen to the Bay of Bengal and potentially plays a role in keeping dissolved oxygen levels in the Bay above the level at which its ecological functioning would be significantly altered.

1 Introduction

Persian Gulf Water (PGW) is an oxygenated, high-salinity water mass that forms in the shallow waters of the Persian Gulf (Figure 1a; Bower, Hunt, & Price, 2000; Prasad,

48 Ikeda, & Prasanna Kumar, 2001), its high salinity a consequence of the very high evap-
49 oration in that region (Prasad et al., 2001; Yao & Johns, 2010). Despite the high degree
50 of mixing that PGW experiences as it passes through the Gulf of Oman and enters the
51 Arabian Sea, this high-salinity, high-oxygen signal is preserved (Figure 1a; Prasad et al.,
52 2001; Vic et al., 2017). PGW is identifiable in the Arabian Sea as a salinity maximum
53 with a density of between 26.2 and 26.8 g kg⁻¹ (Jain et al., 2017; Schott & McCreary,
54 2001) that is distinct from the other high-salinity water masses of the northern Indian
55 Ocean – i.e. Arabian Sea High-Salinity Water (22.8 – 24 kg m⁻³) and Red Sea Water (27 –
56 27.4 kg m⁻³; Jain et al., 2017; Prasanna Kumar & Prasad, 1999). The passage of PGW
57 through the Gulf of Oman and its subsequent spreading in the Arabian Sea are the sub-
58 ject of previous work (e.g. Bower et al., 2000; Ezam, Bidokhti, & Javid, 2010; Prasad et
59 al., 2001; Vic et al., 2017), and the role of PGW in ventilating the Arabian Sea OMZ
60 has been documented (e.g. Lachkar, Lévy, & Smith, 2019; McCreary et al., 2013). The
61 fate of PGW beyond the Arabian Sea has received less attention.

62 The Bay of Bengal (BoB; Figure 1a) is an oxygen minimum zone (OMZ; D’Asaro,
63 Altaet, Suresh Kumar, & Ravichandran, 2020; McCreary et al., 2013), a region of the
64 ocean where low oxygen concentrations (< 60 μmol kg⁻¹) may be harmful to marine life,
65 and where, when oxygen concentrations are very low (< 6 μmol kg⁻¹), biogeochemical
66 cycles may be significantly altered (Queste, Vic, Heywood, & Piontkovski, 2018). The
67 density range of PGW matches the density range of the BoB OMZ (McCreary et al., 2013).
68 OMZs exert an influence on the nitrogen cycle, and hence on the carbon cycle (Gruber,
69 2008), that is disproportionate to their size (Johnson, Riser, & Ravichandran, 2019). Un-
70 derstanding the controls on the location, size and functioning of OMZs is therefore of
71 critical importance, particularly as the extent and intensity of OMZs are predicted to
72 increase over the 21st century due to climate change (e.g. Bopp et al., 2013; Oschlies,
73 Schulz, Riebesell, & Schmitter, 2008).

74 Processes that maintain the BoB OMZ are poorly understood, and it has not been
75 well reproduced in models (McCreary et al., 2013). The strength of stratification in the
76 BoB is such that horizontal oxygen transport from the south is of critical importance
77 (D’Asaro et al., 2020). Johnson et al. (2019) have highlighted the high-degree of vari-
78 ability that dominates the BoB OMZ, and suggest that physical processes resulting in
79 the episodic injection of water with oxygen concentrations between 5 and 10 μmol kg⁻¹
80 keep oxygen concentrations high enough to prevent large-scale denitrification, a chem-

81 ical process that strips bio-available nitrogen from the water column and thus may hin-
82 der phytoplankton growth. Sridevi and Sarma (2020) report that cyclonic and anti-cyclonic
83 eddies can increase and decrease sub-surface oxygen concentrations respectively. Taken
84 together, these results point to a complex relationship between physics and biogeochem-
85 istry in the BoB, with oxygen concentrations depending on multiple processes that of-
86 ten operate over small spatial scales. Although the BoB OMZ is weaker than others in
87 which pronounced denitrification occurs (D’Asaro et al., 2020), it may be close to a tip-
88 ping point: a small reduction in oxygen transport to the OMZ could lead to a large in-
89 crease in denitification (D’Asaro et al., 2020; Johnson et al., 2019). Consequently, un-
90 derstanding the flow of oxygenated water masses into the BoB OMZ is essential for un-
91 derstanding both how the BoB OMZ operates today and how it may respond to a chang-
92 ing climate.

93 Previous studies have disagreed on the presence of PGW in the BoB. Some obser-
94 vational studies have interpreted salinity maxima in the BoB as evidence of PGW (Rochford,
95 1964; Varadachari, Murty, & Reddy, 1968); others have found no such maxima (Shetye
96 et al., 1993, 1991) or else have found no evidence of PGW beyond the Arabian Sea (Kuksa,
97 1972; Quadfasel & Schott, 1982; Shenoi, Shetye, D., & Michael, 1993). Modeling stud-
98 ies of PGW either find no transport to the BoB (Han & McCreary, 2001), or else do not
99 address the question (Durgadoo, Rhs, Biastoch, & Bning, 2017). Most recently, Jain
100 et al. (2017) identified PGW in a dozen temperature, salinity and oxygen profiles from
101 across the BoB; they propose that the Southwest Monsoon Current (SMC; Figure 1 Vinay-
102 achandran, Masumoto, Mikawa, & Yamagata, 1999; Webber et al., 2018), a relatively
103 strong northeastward flow that occurs during the southwest monsoon (June to Septem-
104 ber), is the primary conduit for PGW entering the BoB, but pathways from the Persian
105 Gulf to the BoB, and the timescales of transport, have not been identified. Here, we present
106 a case study of PGW injection into the BoB, from which we determine transport path-
107 ways and timescales from the northern Arabian Sea to the BoB. We use ocean glider ob-
108 servations and 11 years of output from a NEMO ocean reanalysis to examine the injec-
109 tion of PGW into the BoB, and to place our case study into an interannual context. We
110 propose that the episodic injection of trace amounts of PGW into the BoB acts to ven-
111 tilate the BoB OMZ and provide the first estimates of the amount of oxygen that PGW
112 may supply to the BoB OMZ.

2 Glider observations of Persian Gulf Water in the Bay of Bengal

Observations were collected using an ocean glider in the southwestern BoB (8°N , 85.4°E) in July 2016 as part of the Bay of Bengal Boundary Layer Experiment (BoB-BLE; Figure 1a; Vinayachandran et al., 2018; Webber et al., 2018). PGW is observed as a salinity maximum between the 26.2 and 26.8 kg m^{-3} isopycnals (Figure 1b and c), corresponding to depths between approximately 200 and 250 m. The salinity maximum exhibits elevated oxygen concentrations (Figure 1b and c): up to $30 \mu\text{mol kg}^{-1}$, against a background concentration between the 26.2 and 26.8 kg m^{-1} isopycnals of below $10 \mu\text{mol kg}^{-1}$. The oxygen concentration of PGW in the BoB is greatly decreased compared to its oxygen concentration in the Gulf of Oman (approximately $100 \mu\text{mol kg}^{-1}$; Queste et al., 2018), close to its source region, presumably due to mixing with lower-oxygen water masses and biological oxygen consumption. The oxygen sensor malfunctioned approximately halfway through the deployment; temperature and salinity observations without an associated oxygen observations are plotted in gray in Figure 1b and c).

The salinity maximum and elevated oxygen concentration are indicative of the presence of PGW. There is a strong link between absolute salinity and oxygen concentration within the PGW density layer: stronger salinity maxima are associated with higher oxygen concentrations (Figure 1b and c). The background water mass between 26.2 and 26.8 kg m^{-1} in this region is North Indian Central Water (You, 1997), which is typified by low oxygen concentrations. PGW entering the BoB thus increases the oxygen concentration and is likely to be the only source of relatively oxygenated waters for the BoB OMZ between these isopycnals. PGW was not observed by any of the four other BoB-BLE gliders deployed contemporaneously further east along 8°N (not shown; Vinayachandran et al., 2018), which suggests that the inflow was of limited horizontal extent.

PGW may be identified in temperature-salinity space as saline deviations from the background temperature-salinity curve (Figure 1b and c). Whereas previous work has identified a tendency towards higher salinities within the range of PGW densities (Jain et al., 2017), our observations reveal a pronounced and sharply defined local salinity maximum indicative of a PGW layer that is distinct from the layers immediately above and below.

3 Pathways and timescales of Persian Gulf Water transport to the Bay of Bengal

Pathways and timescales of transport between the Persian Gulf and the BoB are investigated using the Nucleus for European Modelling of the Ocean (NEMO) version 3.1 (Madec, 2008) ocean re-analysis. A salinity maximum on the 26.5 kg m^{-3} isopycnal at the time and location of the glider observations is identified in the NEMO output; this closely resembles the signal of PGW found in the glider observations (Figure 1b and c).

Salinity and velocity are linearly interpolated in density space onto the 26.5 kg m^{-3} isopycnal; this isopycnal has previously been taken as the core density of PGW (Bower et al., 2000; Prasad et al., 2001). The salinity maximum is associated with a filament of high-salinity ($> 35.25 \text{ g kg}^{-1}$) water flowing northeastward from the saline waters found south of 4°N to the relatively fresher waters of the BoB (Figure 2). We take this filament to be the feature associated with the PGW intrusion found in our observations. The filament, which is located on the western flank of the SMC and is apparent over a period of approximately one month, evolves in time, extending progressively further northward into the southern BoB, before being caught between a cyclonic eddy to the north and an anti-cyclonic eddy to the south. The filament eventually splits, with the northern part continuing to be advected north (Figure 2). The presence of the filament also demonstrates that PGW advection into the BoB may happen as part of sporadic physical structures rather than being a diffuse phenomenon.

We perform backward-trajectory particle tracking experiments to determine the transport pathways and timescales of water in the filament. We follow the method of Sanchez-Franks et al. (2019). Model velocities on the 26.5 kg m^{-3} isopycnal are bi-linearly interpolated to the particle locations, and the particles are advected using a fourth-order Runge-Kutta scheme with a time step of 12 hours. We assume that diapycnal diffusivity is negligible and that PGW remains at the 26.5 kg m^{-3} isopycnal. Particles are released daily between 24 June and 8 July 2016 inclusive, in a grid pattern at 1 km intervals between 6 and 7°N , and 84 and 86°E (Figure 2b). Not all grid points fall within the plume on all days. A total of 374,640 particles are released and are tracked backwards in time for five years (i.e. to July 2011). Any particle that is found to have a source region north of 20°N in the Arabian Sea is taken to be indicative of PGW transport to the BoB. Note that by source region we refer to the end point of the backward trajectory – that is, the start point of the equivalent forward trajectory. North of 20°N , PGW occupies the en-

176 tire Arabian Sea on the 26.5 kg m^{-3} isopycnal (Prasad et al., 2001; Shenoi et al., 1993).
177 We do not attempt to track particles back to the Persian Gulf, because the complex eddy-
178 topography interactions that occur as PGW exits the Persian Gulf lead to significant di-
179 apycnal mixing in this region (Bower et al., 2000; Vic et al., 2017).

180 Of the backwards-tracked particles, 643 (0.17%) have a source region in the north-
181 ern Arabian Sea. This is consistent with the small volume of PGW observed in the BoB.
182 Two main pathways are identified along which PGW is advected (*forward* in time) from
183 the northern Arabian Sea to the southern BoB (Figure 3b). Following the eastern path-
184 way (*forward* in time), PGW is transported southward along the coast of India, then is
185 transported eastward to the south of Sri Lanka, before entering the BoB (Figure 3b). Fol-
186 lowing the western pathway (*forward* in time), PGW is transported southward along the
187 coasts of Oman and Somalia before turning eastward north of the equator. South of In-
188 dia, at approximately 75°E , it joins up with PGW following the eastern pathway and
189 is similarly transported into the BoB (Figure 3b). These pathways, particularly the west-
190 ern pathway, resemble those identified by Sanchez-Franks et al. (2019) for the transport
191 of Arabian Sea High-Salinity Water to the BoB. This is the first time that the spread-
192 ing of PGW along both sides of the Arabian Sea has been linked to transport to the BoB.
193 All these particle trajectories converge into the SMC; this is to be expected since the par-
194 ticles were released in a plume associated with this current.

195 To determine whether the salinity of the water masses observed align with their
196 source region, we associate each particle with the salinity at the release point of its back-
197 ward trajectory (Figure 2b), interpolated from NEMO data. The mean salinity of par-
198 ticles that have a source region in the northern Arabian Sea (35.30 g kg^{-1}) is higher than
199 that of particles that have a source region elsewhere (35.16 g kg^{-1} ; Figure 3a) and is higher
200 than the 35.25 g kg^{-1} threshold used previously to define the high-salinity filament (Fig-
201 ure 2). The mean salinity of particles that have a source region in the northern Arabian
202 Sea cannot be reproduced by random Monte Carlo sampling ($n = 1,000,000$) of the salin-
203 ity distribution of all released particles. Hence, the particles that have a source region
204 in the northern Arabian Sea are extremely unlikely ($p < 0.001$) to be the result of ran-
205 dom sampling.

206 Using 11 years of NEMO re-analysis (January 2007 to December 2017 inclusive),
207 we perform a forward-trajectory particle tracking experiment to test whether the advec-

208 tion of PGW from the northern Arabian Sea to the BoB is a persistent phenomenon. Par-
209 ticles are released on the first day of every month between January 2007 and December
210 2012 along a transect at 20°N , from the eastern coast of Oman (58°E) to the western
211 coast of India (72°E). Any particle that crosses 8°N between the eastern coast of Sri Lanka
212 and 98°E is considered to be indicative of PGW transport to the BoB. Of the forwards-
213 tracked particles, 0.025% reach the BoB. This indicates that a very small fraction of PGW
214 is transported into the BoB on these time scales. However, even the low concentrations
215 observed here can raise the oxygen concentration on arrival in the BoB (Figure 1b and
216 c). The eastern and western pathways identified in the case study also emerge from the
217 forward trajectories (Figure 3c). The majority (84%) of particles follow the eastern path-
218 way, which suggests that the more equal separation between eastern and western path-
219 ways found for the July 2016 filament was unusual.

220 The first PGW particles in the forward-trajectory experiment arrive in the BoB
221 via the eastern pathway between 1.5 and two years after being released in the northern
222 Arabian Sea (blue colors in Figure 4a); the first particles arrive via the western path-
223 way just under three years after being released (orange colors Figure 4a). The flux of
224 PGW particles into the BoB reaches a maximum between four and five years after re-
225 lease (Figure 4a). The flux of PGW into the BoB is enhanced between May and Septem-
226 ber (Figure 4b) – that is, during the southwest monsoon. The influence of this enhance-
227 ment is seen in the distribution of transport times, being responsible for local peaks in
228 transport time that occur approximately one year apart. The diagonal colored lines in
229 Figure 4a connect transport times that result in particles being advected northwards across
230 8°N during the same southwest monsoon season; the distribution of transport time is
231 better explained by month of entry than by month of release.

232 The range of longitudes at which the majority of these particles enter the BoB dur-
233 ing the southwest monsoon, i.e. between 82 and 87°E (Figure 4b), is consistent with the
234 location of the SMC (Figure 1; Vinayachandran et al., 1999), suggesting that the SMC
235 is the primary feature responsible for advecting PGW into the BoB. The SMC is a surface-
236 intensified current – greatest flow speeds are found in the top 150 m – but climatolog-
237 ical mean northward flow extends to approximately 400 m (Webber et al., 2018). SG579
238 was placed in the eastern portion of this PGW flux region (Figures 1a and 4b). Four other
239 gliders deployed during the BoBBLE campaign were located between 87 and 89°E , at
240 which longitudes relatively fewer PGW particles enter the BoB (Figure 4b); this suggests

241 that the lack of PGW to the east of SG579 was not atypical. Our finding that the SMC
242 is largely responsible for the advection of PGW into the BoB agrees with the hypoth-
243 esis of Jain et al. (2017), but our results also demonstrate that small amounts of PGW
244 enter the BoB at other times of year and at other longitudes, most notably in Decem-
245 ber (Figure 4b).

246 We hypothesise that the transport of PGW between the northern Arabian Sea and
247 the BoB, and the dominance of the eastern pathway, may be explained by the effect of
248 the seasonally reversing currents of the northern Indian Ocean on interannual timescales.
249 Southward flow via the eastern pathway at the depth of the 26.5 kg m^{-3} isopycnal oc-
250 curs during the northeast monsoon in an undercurrent associated with the West India
251 Coastal Current (WICC; Amol et al., 2014); the WICC itself is too shallow (top 100 m)
252 to affect the 26.5 kg m^{-3} isopycnal. The annual cycle of flow in this undercurrent is six
253 months out of phase with flow in the WICC, being northward during the southwest mon-
254 soon and southward during the northeast monsoon (Amol et al., 2014). Despite these
255 semi-annual flow reversals, annual mean flow is southward (Amol et al., 2014). Conse-
256 quently, PGW entrained in this undercurrent, which stretches the full width of the west-
257 ern coast of India (Amol et al., 2014), will be advected southward. That the majority
258 of PGW particles follow this eastern pathway is probably because it represents a more
259 direct route to the BoB. Particles that follow the western pathway in the Arabian Sea
260 are more likely to be advected to other parts of the ocean – for instance the southern
261 Indian Ocean (Durgadoo et al., 2017).

262 **4 Influence of Persian Gulf Water on the Bay of Bengal oxygen min-** 263 **imum zone**

264 Oxygenated PGW entering the BoB throughout the year supports the hypothe-
265 sis proposed by McCreary et al. (2013) and Johnson et al. (2019): that the BoB OMZ
266 is kept at oxygen concentrations above the level at which denitrification occurs by phys-
267 ical processes that sporadically inject relatively oxygenated water. Johnson et al. (2019)
268 propose that eddies are primarily responsible for this flux of oxygenated water, and note
269 that eddies have previously been identified as key transporters of oxygen into other OMZs
270 (e.g. Lachkar, Smith, Lévy, & Pauluis, 2016; Resplandy et al., 2012). The flux of PGW
271 identified here could be a physical process responsible for the ventilation of the BoB OMZ.
272 Johnson et al. (2019) find no seasonality in the BoB OMZ, and it is plausible that the

273 effect of the seasonal enhancement in the PGW flux driven by the SMC is diminished
 274 as PGW is re-distributed and its oxygen consumed.

275 We perform an idealised calculation to produce an order-of-magnitude estimate of
 276 the amount of oxygen, ΔO_{PGW} , supplied to the BoB OMZ by the filament identified in
 277 this study (Figures 1 and 2). We consider a filament that contains PGW and lower-oxygen
 278 ambient water. The mass of the filament, M_{FIL} , is given by:

$$M_{FIL} = W \times H \times U \times \Delta t \times \rho, \quad (1)$$

279 where $W = 100$ km is the width of the high-salinity filament (Figure 2), $H = 100$ m is
 280 its vertical extent (from glider observations; not shown), $U = 0.2$ m s⁻¹ is its speed (Fig-
 281 ure 2), $\Delta t = 15$ days is its duration (from NEMO re-analysis; not shown) and $\rho = 1026.5$ kg m⁻³
 282 is its density (Figure 1). This gives $M_{FIL} = 2.7 \times 10^{15}$ kg. For PGW with an oxygen
 283 concentration of $20 \mu\text{mol kg}^{-1}$ (Figure 1c) and ambient water with an oxygen concen-
 284 tration of $10 \mu\text{mol kg}^{-1}$ (Figure 1c; D'Asaro et al., 2020), PGW provides additional oxy-
 285 gen at $10 \mu\text{mol kg}^{-1}$. Multiplied by mass M_{FIL} , this equates to $\Delta O_{PGW} = 2.7 \times 10^{16}$ μmol .

286 The increase in oxygen concentration effected by ΔO_{PGW} depends on the volume
 287 over which it is re-distributed; if re-distributed over the mass of the entire BoB OMZ,
 288 M_{OMZ} (we assume 1,000 by 1,000 km by 400 m, therefore $M_{OMZ} = 4.1 \times 10^{17}$ kg),
 289 the increase in oxygen concentration resulting from ΔO_{PGW} of this filament would be
 290 $0.07 \mu\text{mol kg}^{-1}$. In more general terms, the additional oxygen supplied by any such fil-
 291 ament is diluted by a factor of $M_{OMZ}/M_{FIL} \approx 150$. However, Johnson et al. (2019)
 292 propose that the BoB OMZ is characterised by its variability rather than its mean state,
 293 and conclude that small changes to the mean state are of limited importance given the
 294 dominance of variability. Consequently ΔO_{PGW} need not be spread over the entire vol-
 295 ume of the BoB OMZ in order to be of biogeochemical significance; in our idealised cal-
 296 culation, this reduces both M_{OMZ} and the dilution factor.

297 Speculating on the volume of the OMZ that is influenced by ΔO_{PGW} is, at present,
 298 necessarily subjective, and a thorough treatment of this question is beyond the scope of
 299 this study. But we note that, Jain et al. (2017) find no evidence of elevated oxygen within
 300 the PGW density range in northern and eastern parts of the BoB. Consequently, we first
 301 assume that PGW is re-distributed over the southwestern corner of the BoB OMZ (500

302 by 500 km). Second, we assume that diapycnal mixing is negligible compared with isopy-
 303 cnal mixing, and the input of ΔO_{PGW} thus retains its original vertical extent (i.e. 100 m).
 304 ΔO_{PGW} would therefore be re-distributed over a mass of 2.6×10^{16} kg and would raise
 305 the oxygen concentration by $1 \mu\text{mol kg}^{-1}$ – i.e. by 20% of the background concentration
 306 in this region (D’Asaro et al., 2020). If additional PGW flux events occur throughout
 307 the year (Figure 4b), our figures will be an underestimate of the influence of PGW on
 308 the BoB OMZ over a year. The oxygen profile from the SMC region (recorded during
 309 the southwest monsoon of 2012) presented by Jain et al. (2017) exhibits a peak of ap-
 310 proximately $30 \mu\text{mol kg}^{-1}$ within the PGW density range, suggesting that the PGW-containing
 311 high-salinity filament we have presented (Figures 1 and 2), and the attendant oxygen flux
 312 we have considered in this section, are not isolated events. Further research is necessary
 313 to accurately quantify the influence of oxygenated PGW on the BoB OMZ.

314 5 Conclusions

315 We have presented observations of a coherent inflow of PGW into the southern BoB.
 316 The flow occurs between the 26.2 and 26.8 kg m^{-3} isopycnals and exhibits the elevated
 317 salinity and oxygen concentration that are characteristic of PGW (Bower et al., 2000;
 318 McCreary et al., 2013; Prasad et al., 2001; Queste et al., 2018). Other water masses be-
 319 tween these isopycnals lack the elevated oxygen concentrations of PGW (You, 1997), sug-
 320 gesting that PGW is likely the only means by which the BoB OMZ may be ventilated
 321 between these isopycnals.

322 The inflow is present in the NEMO ocean reanalysis as a filament of high-salinity
 323 water flowing from the region of high-salinity ($> 35.25 \text{ g kg}^{-1}$) water close to the equa-
 324 tor on 26.5 kg m^{-3} into the fresher waters of the southern BoB. Particle tracking exper-
 325 iments demonstrate that PGW is transported to the BoB principally via the West In-
 326 dia Coastal Current in the eastern Arabian Sea, but also via the western Arabian Sea
 327 and via equatorial currents. Both spreading pathways connect the northern Arabian Sea
 328 to the southern BoB on timescales of longer than two years. Our results reveal a year-
 329 round flux of PGW into the BoB that is enhanced during the southwest monsoon. The
 330 location of this flux, which is predominantly between 82 and 87°E , matches the location
 331 of the SMC, a strong current that flows northward in the BoB at this time.

332 Recent work has focused attention on the highly variable oxygen concentrations
333 in its OMZ and, in contrast to the Arabian Sea, suggests a system dominated by this
334 variability (Johnson et al., 2019). The sporadic injection of PGW into the BoB OMZ,
335 and the associated oxygen supply, has the potential to cause marked local elevations in
336 oxygen concentration and, as such, should be considered alongside features such as ed-
337 dies in future studies of the BoB OMZ. From our observations, we estimate that PGW
338 may deliver approximately 20% of the oxygen in the southwestern BoB OMZ. The PGW
339 layer is predicted to shoal under climate change, as warming of the Gulf increases PGW's
340 core temperature (Lachkar et al., 2019). Any such warming could alter the depth at which
341 PGW enters the BoB, and so reduce ventilation of the BoB OMZ. Given the proxim-
342 ity of the BoB OMZ to the denitrification threshold, any reduction in oxygen could have
343 profound consequences for the biogeochemical and ecological functioning of the BoB and
344 for the global nitrogen cycle.

345 **Acknowledgments**

346 The NERC-funded Bay of Bengal Boundary Layer Experiment supported PMFS, BGMW,
347 AJM and KJH (NE/L013827/1), and ASF (NE/L013835/1). PNV thanks the Ministry
348 of Earth Sciences, Government of India for funding under the BoBBLE project. The Seaglider
349 observations (Webber et al., 2019) are archived at the British Oceanographic Data Cen-
350 tre (www.bodc.ac.uk; doi:10/dgvj). The authors acknowledge the Copernicus Marine En-
351 vironment Monitoring Service for access to NEMO output
352 (available at: <http://marine.copernicus.eu/services-portfolio/access-to-products>), and
353 we are grateful to the NEMO modelling community. We thank the two reviewers for valu-
354 able feedback on earlier drafts of this article.

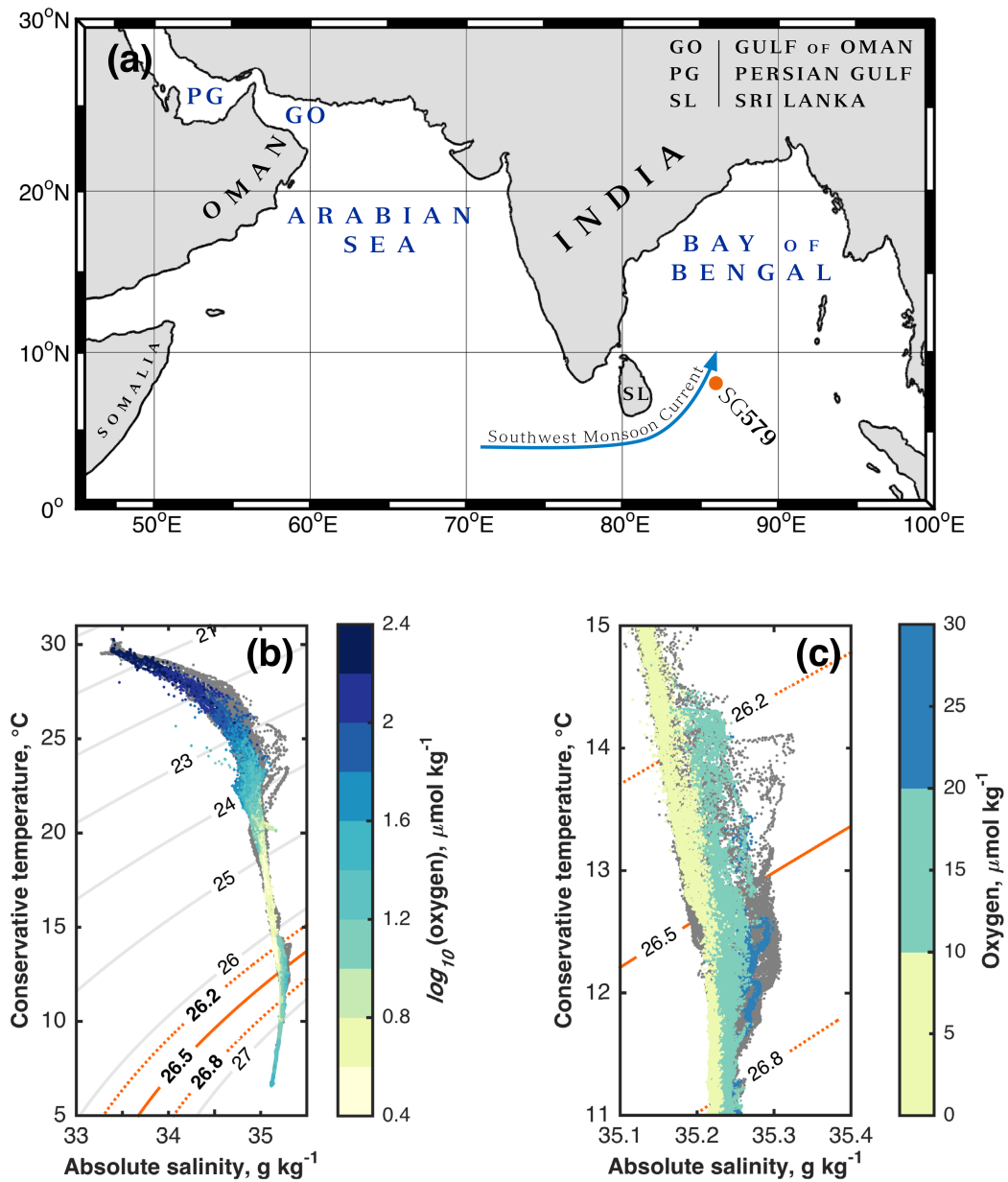
355 **References**

- 356 Amol, P., Shankar, D., Fernando, V., Mukherjee, A., Aparna, S. G., Fernandes, R., . . .
357 Vernekar, S. P. (2014). Observed intraseasonal and seasonal variability of the West
358 India Coastal Current on the continental slope. *Journal of Earth System Science*,
359 *123*, 1045 – 1074.
- 360 Bopp, L., Resplandy, L., Orr, J. C., Doney, S. C., Dunne, J. P., Gehlen, M., . . . Vichi, M.
361 (2013). Multiple stressors of ocean ecosystems in the 21st century: projections with
362 CMIP5 models. *Biogeosciences*, *10*, 6255 – 6245.

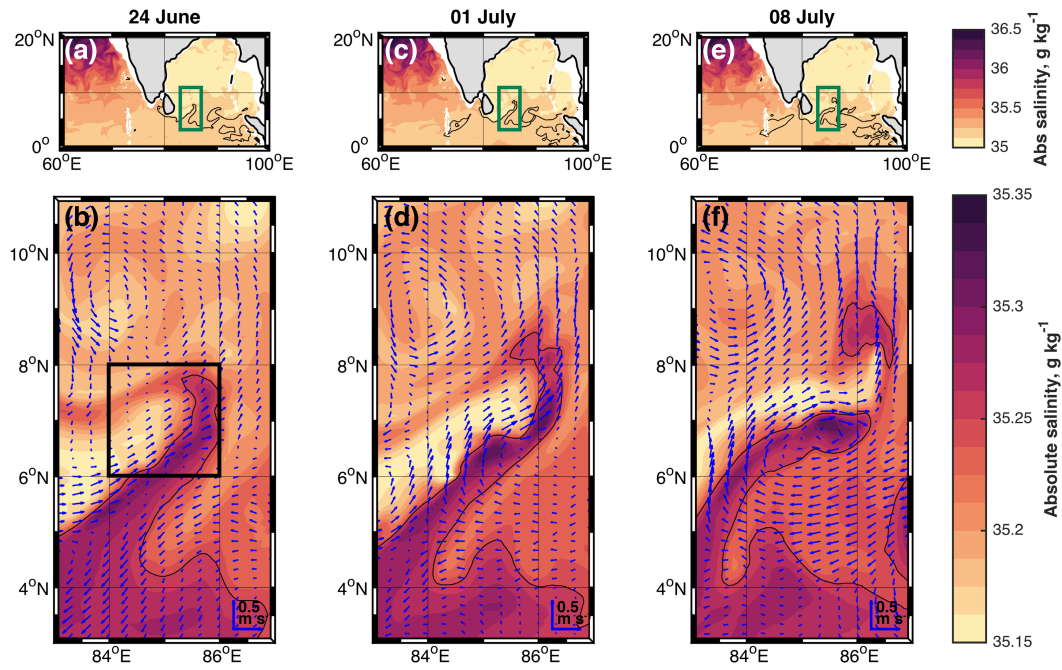
- 363 Bower, A. S., Hunt, H. D., & Price, J. F. (2000). Character and dynamics of the Red Sea
364 and Persian Gulf outflows. *Journal of Geophysical Research*, *105*, 6387 – 6414.
- 365 D’Asaro, E., Altaet, M., Suresh Kumar, N., & Ravichandran, M. (2020). Structure of the
366 Bay of Bengal oxygen deficient zone. *Deep-Sea Research II*,
367 doi.org/10.1016/j.dsr2.2019.104650.
- 368 Durgadoo, J. V., Rühs, S., Biastoch, A., & Böning, C. W. B. (2017). Indian Ocean
369 sources of Agulhus leakage. *Journal of Geophysical Research: Oceans*, *122*,
370 3481 – 3499.
- 371 Ezam, M., Bidokhti, A. A., & Javid, A. H. (2010). Numerical simulations of spreading of
372 the Persian Gulf outflow into the Oman Sea. *Ocean Science*, *6*, 887 – 900.
- 373 Gruber, N. (2008). The marine nitrogen cycle: overview and challenges. In D. G. Capone,
374 D. A. Bronk, M. R. Mulholland, & E. J. Carpenter (Eds.), *Nitrogen in the marine*
375 *environment* (pp. 1 – 50). Burlington, United States of America.
- 376 Han, W., & McCreary, J. P. (2001). Modelling salinity distributions in the Indian Ocean.
377 *Journal of Geophysical Research*, *106*, 859 – 877.
- 378 Jain, V., Shankar, D., Vinayachandran, P. N., Kankonkar, A., Chatterjee, A., Amol, P.,
379 ... Neema, C. P. (2017). Evidence for the existence of Persian Gulf Water and Red
380 Sea Water in the Bay of Bengal. *Climate Dynamics*, *48*, 3207 – 3226.
- 381 Johnson, K. S., Riser, S. C., & Ravichandran, M. (2019). Oxygen variability controls
382 denitrification in the Bay of Bengal oxygen minimum zone. *Geophysical Research*
383 *Letters*, *46*, 804 – 811.
- 384 Kuksa, V. I. (1972). Some peculiarities of the formation and distribution of intermediate
385 layers in the Indian Ocean. *Oceanology*, *12*, 21 – 30.
- 386 Lachkar, Z., Lévy, M., & Smith, S. (2019). Strong intensification of the Arabian Sea
387 oxygen minimum zone in response to Arabian Gulf warming. *Geophysical Research*
388 *Letters*, *46*, 5420 – 5429.
- 389 Lachkar, Z., Smith, S., Lévy, M., & Pauluis, O. (2016). Eddies reduce denitrification and
390 compress habitats in the Arabian Sea. *Geophysical Research Letters*, *43*,
391 9148 – 9156.
- 392 Madec, G. (2008). *NEMO ocean engine. Note du Pôle de modélisation* (Tech. Rep. No.
393 27. ISSN no 1288-1619). France: Institute Pierre-Simon Laplace.
- 394 McCreary, J. P., Z., Y., Hood, R. R., Vinayachandran, P. N., Furue, R., Ishida, A., &
395 Richards, K. J. (2013). Dynamics of the Indian Ocean oxygen minimum zones.

- 396 *Progress in Oceanography*, 112-113, 15 – 37.
- 397 Oschlies, A., Schulz, K. G., Riebesell, U., & Schmitter, A. (2008). Simulated 21st
398 century's increase in oceanic suboxia by CO₂-enhanced biotic carbon export. *Global*
399 *Biogeochemical Cycles*, 22, GB4008.
- 400 Prasad, T. G., Ikeda, M., & Prasanna Kumar, S. (2001). Seasonal spreading of the
401 Persian Gulf water mass in the Arabian Sea. *Journal of Geophysical Research*, 106,
402 17059 – 17071.
- 403 Prasanna Kumar, S., & Prasad, T. G. (1999). Formation and spreading of Arabian Sea
404 high-salinity water mass. *Journal of Geophysical Research*, 104, 1455 – 1464.
- 405 Quadfasel, D., & Schott, F. (1982). Water mass distributions at intermediate layers off
406 the Somali coast during the onset of the southwest monsoon. *Journal of Physical*
407 *Oceanography*, 12, 1358 – 1372.
- 408 Queste, B. Y., Vic, C., Heywood, K. J., & Piontkovski, S. A. (2018). Physical controls on
409 oxygen distribution and denitrification potential in the northwest Arabian Sea.
410 *Geophysical Research Letters*, 45, 4143 – 4152.
- 411 Resplandy, L., Lévy, M., Bopp, L., Echevin, V., Pous, Sarma, V. V. S. S., & Kumar, D.
412 (2012). Controlling factors of the oxygen balance in the Arabian Sea's OMZ.
413 *Biogeosciences*, 9, 5095 – 5109.
- 414 Rochford, D. J. (1964). Salinity maxima in the upper 1000 metres of the North Indian
415 Ocean. *Australian Journal of Marine and Freshwater Research*, 15, 1 – 24.
- 416 Sanchez-Franks, A., Webber, B. G. M., King, B. A., Vinayachandran, P. N., Matthews,
417 A. J., Sheehan, P. M. F., ... Neema, C. P. (2019). The railroad switch effect of
418 seasonally reversing currents on the Bay of Bengal high-salinity core. *Geophysical*
419 *Research Letters*, 46, 6005 – 6014.
- 420 Schott, F. A., & McCreary, J. P. (2001). The monsoon circulation of the Indian Ocean.
421 *Progress in Oceanography*, 51, 1 – 123.
- 422 Shenoi, S. S. C., Shetye, S. R., D., G. A., & Michael, G. S. (1993). Salinity extrema in the
423 Arabian Sea. In V. Ittekkot & R. R. Nair (Eds.), *Monsoon Biogeochemistry* (pp.
424 37 – 49). Hamburg, Germany: University of Hamburg.
- 425 Shetye, S. R., D., G. A., Shenoi, S. S. C., Sundar, D., Michael, G. S., & Nampoothiri, G.
426 (1993). The western boundary current of the seasonal subtropical gyre in the Bay of
427 Bengal. *Journal of Geophysical Research*, 98, 945 – 954.
- 428 Shetye, S. R., Shenoi, S. S. C., D., G. A., Michael, G. S., Sundar, D., & Nampoothiri, G.

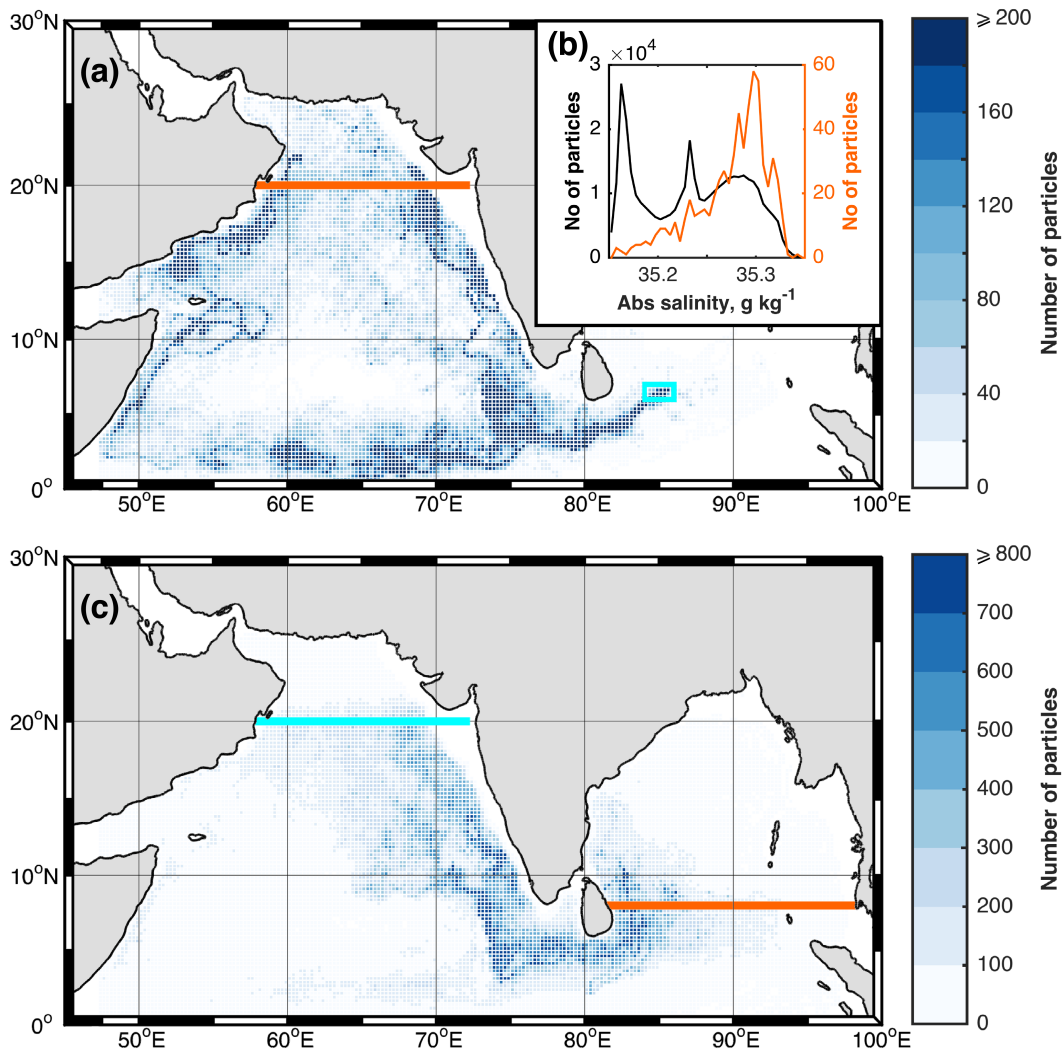
- 429 (1991). Wind-driven coastal upwelling along the western boundary of the Bay of
430 Bengal during the southwest monsoon. *Continental Shelf Research*, *11*, 1397 – 1408.
- 431
- 432 Sridevi, B., & Sarma, V. V. S. S. (2020). A revisit to the regulation of the oxygen
433 minimum zone in the Bay of Bengal. *Journal of Earth System Science*, *129*, 107.
- 434 Varadachari, V. V. R., Murty, C. S., & Reddy, C. V. G. (1968). Salinity maxima
435 associated with some sub-surface water masses in the upper layers of the Bay of
436 Bengal. *Bulletin of the National Institute of Sciences of India*, *38*, 338 – 343.
- 437 Vic, C., Rouillet, G., Capet, X., Carton, X., Molemaker, M. J., & Gula, J. (2017).
438 Eddy-topography interactions and the fate of the Persian Gulf outflow. *Journal of*
439 *Geophysical Research: Oceans*, *120*, 6700 – 6717.
- 440 Vinayachandran, P. N., Masumoto, Y., Mikawa, T., & Yamagata, T. (1999). Intrusion of
441 the Southwest Monsoon Current into the Bay of Bengal. *Journal of Geophysical*
442 *Research*, *104*, 11077 – 11085.
- 443 Vinayachandran, P. N., Matthews, A. J., Vijay Kumar, K., Sanchez-Franks, A., Thushara,
444 V., George, J., ... Joshi, M. (2018). BoBBLE (Bay of Bengal Boundary Layer
445 Experiment): ocean-atmosphere interaction and its impact of the South Asian
446 monsoon. *Bulletin of the American Meteorological Society*, *99*, 1569 – 1587.
- 447 Webber, B. G. M., Matthews, A. J., Queste, B. Y., Lee, G. A., Cobas-Garcia, M.,
448 Heywood, K. J., & Vinayachandran, P. N. (2019). Ocean glider data from five
449 Seagliders deployed in the Bay of Bengal during the BoBBLE (Bay of Bengal
450 Boundary Layer Experiment) project in July 2016. *British Oceanographic Data*
451 *Centre, National Oceanography Centre, NERC, DOI: doi:10/dgvj*.
- 452 Webber, B. G. M., Matthews, A. J., Vinayachandran, P. N., Neema, C. P.,
453 Sanchez-Franks, A., Vijith, V., ... Baranowski, D. B. (2018). The dynamics of the
454 Southwest Monsoon Current in 2016 from high-resolution observations and models.
455 *Journal of Physical Oceanography*, *48*, 2259 – 2282.
- 456 Yao, F., & Johns, W. E. (2010). A HYCOM modelling study of the Persian Gulf: 2.
457 formation and export of Persian Gulf Water. *Journal of Geophysical Research*, *115*,
458 C11018.
- 459 You, Y. (1997). Seasonal variations of thermocline circulation and ventilation in the
460 Indian Ocean. *Journal of Geophysical Research*, *102*, 10391 – 10422.



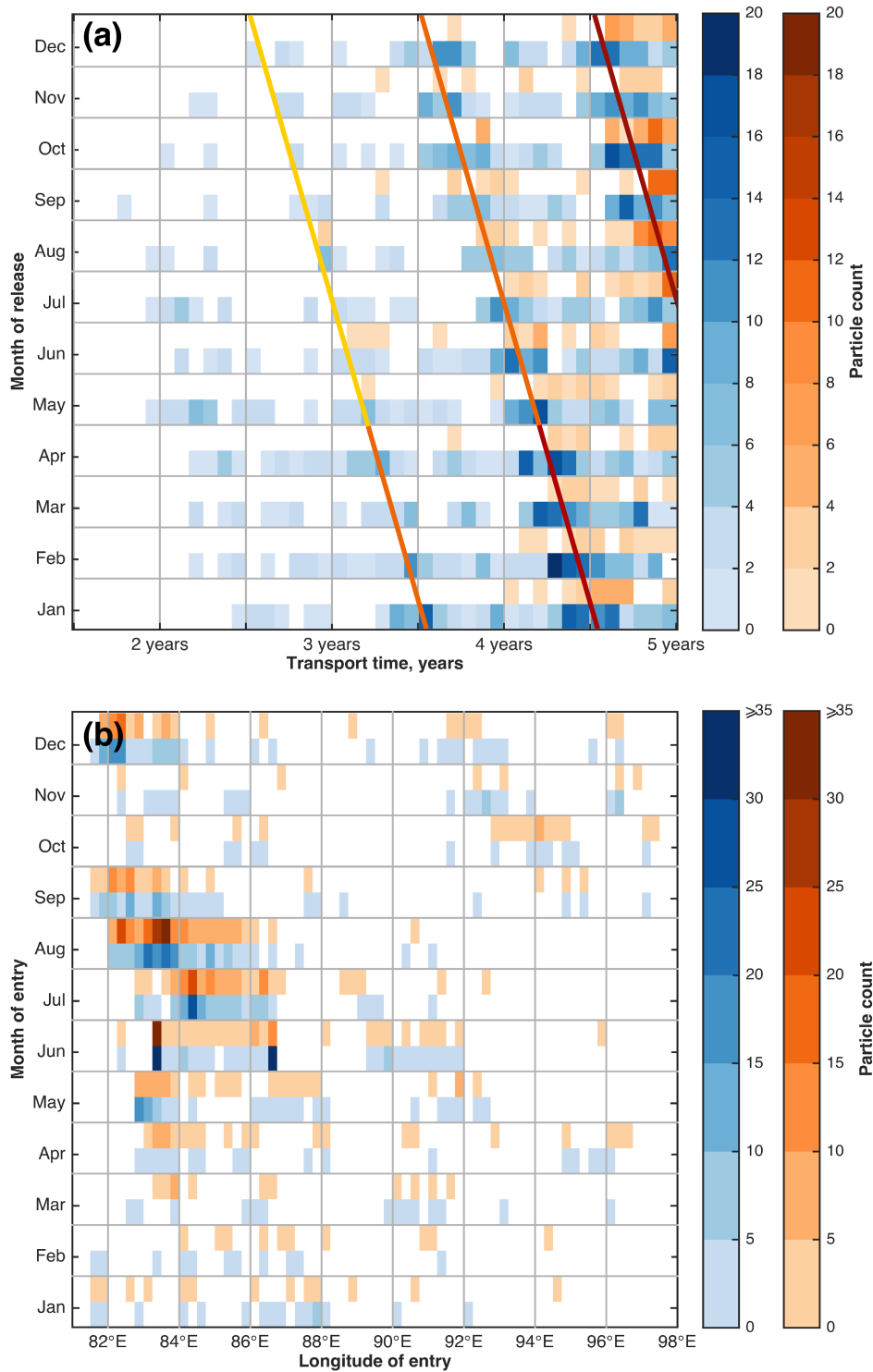
461 **Figure 1.** (a) Map of the northern Indian Ocean, showing the location of Seaglider (SG)
 462 579. The approximate path of the Southwest Monsoon Current (Vinayachandran et al., 1999)
 463 is shown by the blue arrow. (b) Temperature-salinity plot of glider observations colored by the
 464 logarithm of oxygen concentration ($\mu\text{mol kg}^{-1}$). (c) As panel (b), but zoomed-in to the Persian
 465 Gulf Water density range, and colored by oxygen concentration ($\mu\text{mol kg}^{-1}$). The oxygen sensor
 466 was not operational for all dives: gray dots indicate temperature and salinity observations that
 467 lack a corresponding oxygen observation.



468 **Figure 2.** Absolute salinity on the 26.5 kg m^{-3} density surface in the NEMO re-analysis on
 469 (a) and (b) 24 June, (c) and (d) 1 July, (e) and (f) 8 July 2016. The area mapped in the
 470 bottom panels is indicated by the green boxes in the top panels. The 35.25 g kg^{-1} isohaline is
 471 indicated by the black contour in all panels. Arrows indicate velocity. The black box in panel (b)
 472 indicates the location of the particle release for the backward-trajectory experiments.



473 **Figure 3.** (a) Number of particles that pass through quarter-degree latitude-longitude bins
 474 during the backward-trajectory experiment. Particles that remain in a bin over consecutive time
 475 steps are not counted twice, but particles that enter, exit, then re-enter a bin are counted twice.
 476 Only particles that cross 20°N in the northern Arabian Sea (orange line) are included. The re-
 477 lease site is enclosed within the light blue box. (b) Distribution of the initial salinity (i.e. salinity
 478 at release) of particles in the backward-trajectory experiment that do not reach the northern
 479 Arabian Sea (black line, left-hand axis) and of particles that do reach the northern Arabian
 480 Sea (orange line, right-hand axis). (c) As for (a), but for the forward-trajectory experiments,
 481 in which particles were released along 20°N in the northern Arabian Sea (light blue line) and
 482 tracked forwards in time to 8°N in the BoB (orange line).



483 **Figure 4.** (a) The time taken for forwards-tracked particles to reach 8°N in the BoB (one-
 484 month bins), by month of release. Particles following the eastern pathway (blue colors) are
 485 analysed separately to those following the western pathway (orange colors). The colored lines join
 486 transport times that result in particles crossing 8°N in the BoB during the third SW monsoon
 487 (yellow), fourth SW monsoon (orange), fifth SW monsoon (red) after release. (b) The number of
 488 forwards-tracked particles crossing 8°N by month and by longitude (0.25° bins).